# Oscillatory mean-field dynamos with a spherically symmetric, isotropic helical turbulence parameter $\alpha$

Frank Stefani* and Gunter Gerbeth†
*Forschungszentrum Rossendorf, P.O. Box 510119, D-01314 Dresden, Germany*
(Received 18 October 2002; published 18 February 2003)

Until recently, the existence of oscillatory mean-field dynamos of the $\alpha^2$ type with spherically symmetric and isotropic turbulence parameter $\alpha$ was an open question. We find such dynamos by means of an evolutionary strategy, and we illustrate the spectral properties of the corresponding dynamo operators.

DOI: 10.1103/PhysRevE.67.027302 PACS number(s): 47.65.+a, 52.65.Kj, 91.25.Cw

For decades, homogeneous dynamos have been the subject of purely theoretical research that tried to explain magnetic field generation in such inaccessible regions as the Earth's deep interior, the Sun's convection zone, or the spiral arms of galaxies. In 1999, this situation has changed with the first successful dynamo experiments at the sodium facilities in Riga [1,2] and Karlsruhe [3,4]. Now, dynamos run in laboratory, and their kinematic behavior can be predicted with an error margin of a few percent [5]. Dynamo theory is not unaffected by those developments in dynamo ''engineering.'' Whereas in the past the relevance of a dynamo model was ultimately judged by its applicability to real cosmic bodies, it is now sensible to ''tailor'' particular models which could show interesting features, e.g., field reversals or mode switching, in the laboratory.

These developments give also new impetus on spectral analysis of dynamo operators. One of the simplest dynamo models is a mean-field dynamo with a spherically symmetric and isotropic helical turbulence parameter $\alpha$. In particular, the case with constant $\alpha$ is one of the rare models in dynamo theory that can be solved semianalytically [6,7]. Though the construction of a spherically symmetric, isotropic $\alpha^2$ dynamo seems away from realistic cosmic dynamos with their, for instance, typical antisymmetry with respect to the equatorial midplane, the basic analysis of this simplest case of $\alpha^2$ dynamos is a necessary starting point for the investigation of more realistic dynamos. Despite its simplicity, the spherically symmetric, isotropic $\alpha^2$ dynamo exhibits a rich spectral structure if $\alpha$ is allowed to vary with the radius [8,9]. In particular, complex eigenvalues have been found for a number of models [9–12]. However, it always turned out that other modes with higher degrees $l$ of the spherical harmonics had larger growth rates than the considered oscillatory mode (cf. Ref. [13]). An explicit example of a spherically symmetric, isotropic $\alpha^2$ dynamo with the dominating mode being oscillatory does not exist up to present.

Thus motivated, our concrete goal in the present paper is to solve the following inverse problem: Find, for an $\alpha^2$ dynamo with spherically symmetric, isotropic $\alpha$, a radial dependence $\alpha(r)$ so that the eigenmode for $l=1$ has zero growth rate and nonzero frequency and that all other modes have negative growth rates. This task fits into a class of recently treated inverse problems concerning the determination of $\alpha(r)$ from the demand that certain spectral properties (a few given eigenvalues [8,9]) or spatial properties of the magnetic field (''hidden dynamos,'' [14]) are fulfilled.

In the following, we will shortly describe the forward solver that is used for the determination of the eigenvalues, and the evolutionary strategy (ES) which we employ to solve the inverse problem formulated above.

We start with the induction equation for a mean-field dynamo model with a spherically symmetric $\alpha$ coefficient (for the basics of mean-field dynamos, see Ref. [7]). Inside a sphere of radius $R$ the electrical conductivity $\sigma$ is constant, whereas it is zero in the exterior. In the interior of the sphere the magnetic field $\boldsymbol{B}$ has to satisfy the induction equation

$$\frac{\partial \boldsymbol{B}}{\partial t} = \boldsymbol{\nabla} \times (\alpha \boldsymbol{B}) + \frac{1}{\mu_0 \sigma} \Delta \boldsymbol{B} \tag{1}$$

and the source-free condition

$$\boldsymbol{\nabla} \cdot \boldsymbol{B} = 0. \tag{2}$$

At the boundary $r=R$, the magnetic field has to match continuously to a potential field in the exterior.

As usual [7], we decompose $\boldsymbol{B}$ into a poloidal and a toroidal part,

$$\boldsymbol{B} = -\boldsymbol{\nabla} \times (\boldsymbol{r} \times \boldsymbol{\nabla} S) - \boldsymbol{r} \times \boldsymbol{\nabla} T, \tag{3}$$

with the defining scalars $S$ and $T$ expanded in spherical harmonics according to

$$S(r,\theta,\phi) = \sum_{l=1}^{\infty} \sum_{m=-l}^{l} R s_l^m(r) Y_l^m(\theta,\phi) \exp(\lambda_l t), \tag{4}$$

$$T(r,\theta,\phi) = \sum_{l=1}^{\infty} \sum_{m=-l}^{l} t_l^m(r) Y_l^m(\theta,\phi) \exp(\lambda_l t). \tag{5}$$

For the remainder of the paper, we will measure the length in units of $R$, the time in units of $\mu_0 \sigma R^2$, and the parameter $\alpha$ in units of $(\mu_0 \sigma R)^{-1}$.

Using Eqs. (3)–(5), the induction equation (1) can be transformed into the eigenvalue equation system:

*Electronic address: F.Stefani@fz-rossendorf.de
†Electronic address: G.Gerbeth@fz-rossendorf.de

 

$$\lambda_{l,n}s_l=\frac{1}{r}\frac{d^2}{dr^2}(rs_l)-\frac{l(l+1)}{r^2}s_l+\alpha(r)t_l, \tag{6}$$

$$\lambda_{l,n}t_l=\frac{1}{r}\frac{d}{dr}\left(\frac{d}{dr}(rt_l)-\alpha(r)\frac{d}{dr}(rs_l)\right)-\frac{l(l+1)}{r^2}[t_l - \alpha(r)s_l]. \tag{7}$$

In our particular case of a spherically symmetric, isotropic $\alpha$ there is no coupling between field modes differing in the degree $l$ of the spherical harmonics. The order $m$ of the coefficients of the defining scalars has been skipped as it does not show up in the equations. The radial wave number is labeled by the index $n$.

The boundary conditions at $r=1$ are as follows:

$$\left.\frac{ds_l}{dr}\right|_{r=1}+(l+1)s_l(1)=t_l(1)=0. \tag{8}$$

A shooting technique and a fifth-order Runge-Kutta method were used to solve this system numerically, utilizing and adapting standard routines from Ref. [15]. This code has been validated by comparison with exact results (available only for $\alpha=$const), and with the results of other codes, including an integral equation solver [16].

For the description of the inverse spectral solver we will be very short, as it has been described in detail in Refs. [8,9]. We use an ES, with a ''population'' of ''individuals'' [parameter vectors that describe the function $\alpha(r)$] evolving in a ''fitness'' landscape according to principles taken from biology. Finally, the evolution is stopped when the population has gathered in the (hopefully) global maximum of the fitness landscape. Note that in every step of the evolution the eigenvalue equation system (6)–(8) is solved correctly, without any compromise with other functionals to be minimized.

This evolutionary strategy is very robust, and it can easily be used for the solution of different inverse spectral problems [8,9]. For the solution of our task we define the fitness $F[\alpha]$ of a function $\alpha(r)$ according to

$$\begin{aligned}F[\alpha]=&-[\mathrm{Re}(\lambda_{1,1}[\alpha])]^2\\&-(1+\epsilon+\tanh\{\mathrm{Im}(\lambda_{1,1}[\alpha])-f\})^{-1}\\&-(1+\epsilon+\tanh\{-\mathrm{Re}(\lambda_{2,1}[\alpha])\})^{-1}\\&-(1+\epsilon+\tanh\{-\mathrm{Re}(\lambda_{3,1}[\alpha])\})^{-1}.\end{aligned} \tag{9}$$

What is the motivation for this choice of the fitness? The first term, to begin with, tries to keep the growth rate $\mathrm{Re}(\lambda_{1,1}[\alpha])$ of the eigenmode with $(l=1|n=1)$ as close as possible to zero. The second term makes the frequency $\mathrm{Im}(\lambda_{1,1}[\alpha])$ of this mode repel from the parameter $f$ which will be considered as variable. The third and the fourth terms are chosen so as to force the growth rates for $(l=2|n=1)$ and $(l=3|n=1)$ to be less than zero. In a strict sense one should also demand the growth rates for all the higher values of $l$ and $n$ to be less than zero, but this can also be checked *a posteriori*. The small value $\epsilon$, which is only used to avoid numerical overflows, is chosen as $10^{-6}$.

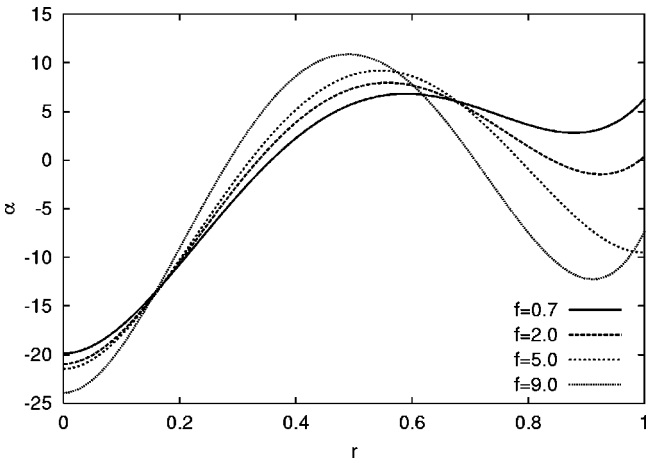


FIG. 1. The functions $\alpha(r)$ resulting from the evolutionary strategy with fitness function $F[\alpha]$ according to Eq. (9) for four different values of $f$.

It should be mentioned that the ES can be combined with a certain regularization of the functions $\alpha(r)$. By means of a regularization parameter we can adjust the allowed mean quadratic curvature of $\alpha(r)$ [8]. It turns out that if we start with a large regularization parameter that keeps the mean quadratic curvature of $\alpha(r)$ small, we do not get any solution of our problem. Only with a rather small regularization parameter that allows more curvature of $\alpha(r)$ the ES yields solutions.

In Fig. 1 we represent, for four different values of the parameter $f$, the functions $\alpha(r)$ resulting as solutions of the ES. Note that the functions $\alpha(r)$ change their sign at least once. As we started with large regularization parameters without getting solutions, the curves in Fig. 1 can be considered as the ''simplest'' ones (in the sense of minimal mean quadratic curvature) that fulfill our spectral demands. The analytical expressions for the curves are given in the following table:

| $f$ | $\alpha(r)$ |
|---|---|
| 0.7 | $-19.88+347.37\,r^2-656.71\,r^3+335.52\,r^4$ |
| 2.0 | $-20.95+399.40\,r^2-765.69\,r^3+387.61\,r^4$ |
| 5.0 | $-21.46+426.41\,r^2-806.73\,r^3+392.28\,r^4$ |
| 9.0 | $-23.93+594.35\,r^2-1243.02\,r^3+665.27\,r^4$ |

For these functions $\alpha(r)$, the growth rates of the eigenmodes with $(l=1,\ldots,3|n=1)$ and the frequency of the eigenmode with $(l=1|n=1)$ are as follows:

| $f$ | $\mathrm{Re}(\lambda_{1,1}[\alpha])$ | $\mathrm{Im}(\lambda_{1,1}[\alpha])$ | $\mathrm{Re}(\lambda_{2,1}[\alpha])$ | $\mathrm{Re}(\lambda_{3,1}[\alpha])$ |
|---|---|---|---|---|
| 0.7 | 0.00 | 4.98 | −5.08 | −12.02 |
| 2.0 | 0.00 | 6.02 | −5.35 | −13.02 |
| 5.0 | 0.01 | 7.24 | −3.64 | −10.82 |
| 9.0 | −0.11 | 9.30 | −1.42 | −9.32 |

These values have been validated in an *a posteriori* analysis of the spectrum for the functions $\alpha(r)$.

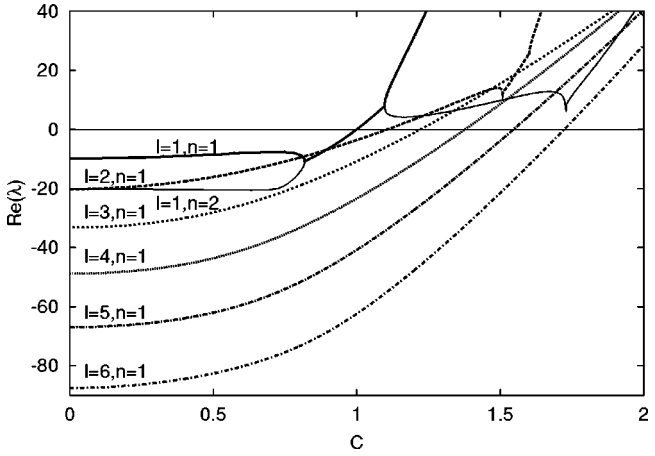


FIG. 2. Special case $f=5.0$. Growth rates for the eigenfunctions with $(l=1|n=1,2)$ and $(l=2,\ldots,6|n=1)$.

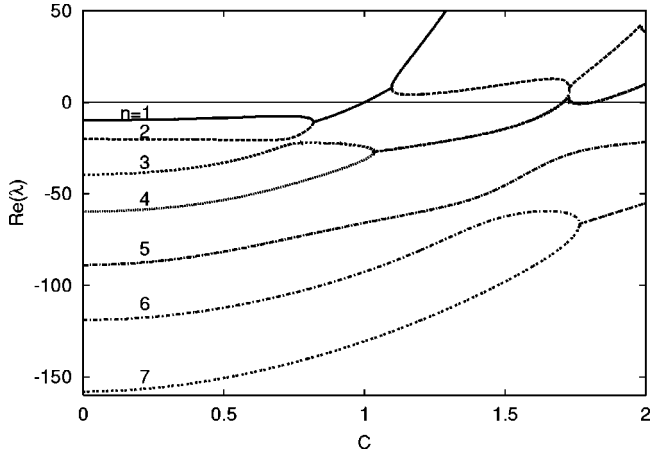


FIG. 4. Special case $f=5.0$. Growth rates for the eigenfunctions with $(l=1|n=1,\ldots,7)$.

Evidently, the ES delivers functions $\alpha(r)$ that fulfill the spectral demands formulated above. The $(l=1|n=1)$ eigenmode with zero growth rate is oscillatory, while the remaining eigenmodes have growth rates less than zero. To be on the safe side, we have also computed the growth rates for modes with $l>3$, which also turned out to be less than zero.

For the sake of illustration, let us concentrate in the following on the spectral properties for the special case with $f=5$. In Fig. 2, we show the growth rates for the eigenmodes with $(l=1|n=1,2)$ and $(l=2,\ldots,6|n=1)$ as functions of $C$, which is used to scale the magnitude of $\alpha(r)$ [for $C=0$ we have the free decay case, $C=1$ corresponds to the obtained functions $\alpha(r)$]. Details of this plot close to the critical point $C=1$ are shown in Fig. 3.

At $C=0$, all modes start as nonoscillatory modes (with purely real eigenvalues). At $C=0.818$, the two modes with $(l=1|n=1)$ and $(l=1|n=2)$ merge and continue as a pair with complex conjugate eigenvalues (only a single line is shown). Interestingly enough, at $C=1.097$ this pair splits off again and the two modes with $(l=1|n=1)$ and $(l=1|n=2)$ continue separately, again with purely real eigenvalues. In between, at $C=1.00$ the pair crosses the abscissa, hence dynamo action occurs. All modes with higher $l$ and $n$ have still negative growth rates at $C=1.00$.

In Figs. 4 and 5, the growth rates and frequencies for the modes with $(l=1|n=1,\ldots,7)$ are plotted. These figures give a flavor of the complexity of the spectrum, with its merging and splitting points of modes with different $n$.

In this respect, another aspect should be addressed. Whereas the spectra for the functions $\alpha(r)$ for $f=0.7,2.0,5.0$ are rather similar, there is a transition if we go to $f=9.0$. Figure 6 shows the corresponding spectrum. Whereas in Fig. 4 we observed a merging of the modes with $n=1$ and $n=2$, we get now a merging of the modes with $n=2$ and $n=3$. For larger $C$, the modes with $n=1$ and $n=4$ come together, meeting at the same point with the common line of the complex conjugated $n=2(3)$ modes.

Evidently, the dynamo operators connected with the obtained functions $\alpha(r)$ show very interesting spectral features which warrants further analysis.

A complete characterization of the $\alpha(r)$ profiles that fulfill our spectral demands would require an extensive parameter study. At least we can get a certain feeling on the broad-

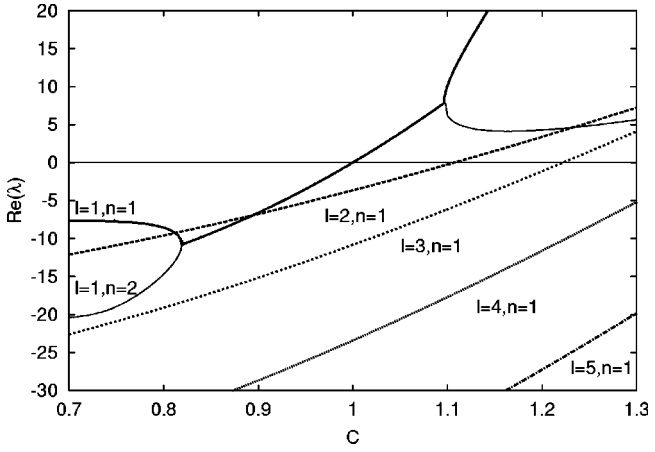


FIG. 3. Special case $f=5.0$. Growth rates for the eigenfunctions with $(l=1|n=1,2)$ and $(l=2,\ldots,5|n=1)$. Details close to the critical point $C=1$.

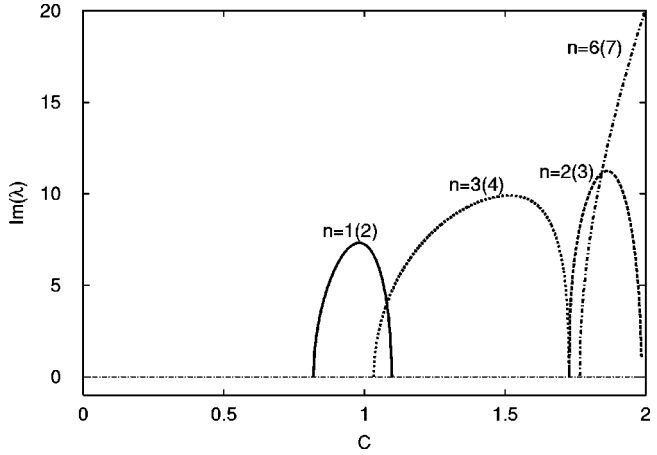


FIG. 5. Special case $f=5.0$. Frequencies for the eigenfunctions with $(l=1|n=1,\ldots,7)$.

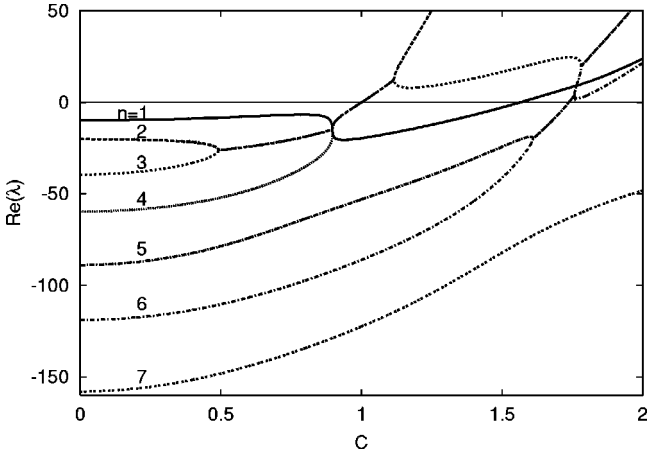


FIG. 6. Special case $f=9.0$. Growth rates for the eigenfunctions with $(l=1|n=1,\ldots,7)$.

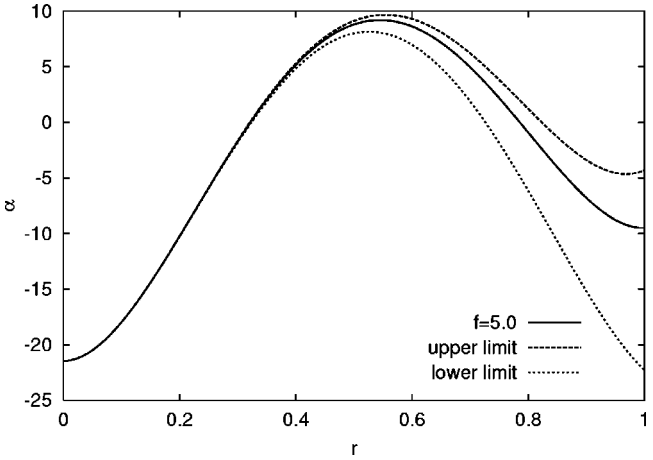


FIG. 7. Modified functions $\alpha(r)$ of the type obtained for $f=5$, but with varying coefficient of the $r^4$ term, which are oscillatory dynamos.

ness of the ''corridor'' for a limited type of deformations. For this purpose, we start with the function $\alpha(r)=-21.46+426.41r^2-806.73r^3+392.28r^4$ which was the solution for $f=5$. Now let us change the coefficient of the $r^4$ term, leaving all other coefficients unchanged. Figure 7 shows the upper and the lower limits of the corresponding deformations that still belong to our oscillatory class of dynamos. Above the upper limit, the $(l=2|n=1)$ mode starts to dominate. Below the lower limit, the $(l=4|n=1)$ mode dominates.

In summary, we have found a class of oscillatory mean-field dynamos with spherically symmetric, isotropic turbulence parameter $\alpha$ working in a finite volume with homogeneous conductivity. The obtained functions $\alpha(r)$ are smooth and by no means exotic or of a pronounced layer type [10,11], but they are characterized by at least one change of sign along the radius. In the sense of minimal averaged quadratic curvature, our solutions seem to be the simplest ones.

As for the back-reaction regime, an interesting behavior of the considered dynamo models is conceivable. Even a slight modification of the functions $\alpha(r)$ due to the action of the Lorentz forces could trigger a transition to a nonoscillatory mode (either with $l=1$ or with higher $l$).

We do not claim any particular astrophysical relevance of our result. However, keeping in mind that the Karlsruhe dynamo experiment is an $\alpha^2$ dynamo (although with an anisotropic $\alpha$ tensor) one could imagine a generalization of our method to similar laboratory dynamos.

[1] A. Gailitis *et al.*, Phys. Rev. Lett. **84**, 4365 (2000).
[2] A. Gailitis *et al.*, Phys. Rev. Lett. **86**, 3024 (2002).
[3] U. Müller and R. Stieglitz, Naturwissenschaften **87**, 381 (2000).
[4] R. Stieglitz and U. Müller, Phys. Fluids **13**, 561 (2001).
[5] A. Gailitis, O. Lielausis, E. Platacis, G. Gerbeth, and F. Stefani, Rev. Mod. Phys. **74**, 973 (2002).
[6] F. Krause and M. Steenbeck, Z. Naturforsch. A **22A**, 671 (1967).
[7] F. Krause and K.-H. Rädler, *Mean-field Magnetohydrodynamics and Dynamo Theory* (Akademie-Verlag, Berlin, 1980).
[8] F. Stefani and G. Gerbeth, Astron. Nachr. **321**, 235 (2000).
[9] F. Stefani and G. Gerbeth, Phys. Earth Planet. Inter. **128**, 109 (2001).
[10] K.-H. Rädler (unpublished).
[11] K.-H. Rädler and H.-J. Bräuer, Astron. Nachr. **308**, 101 (1987).
[12] G. Schubert and K. Zhang, Astrophys. J. Lett. **532**, L149 (2000).
[13] G. Rüdiger, D. Elstner, and M. Ossendrijver, e-print astro-ph/0212203.
[14] R. Kaiser and A. Tilgner, Phys. Rev. E **63**, 037301 (2001).
[15] W. H. Press, S. A. Teukolsky, W. T. Vetterling, and B. F. Flannery, *Numerical Recipes* (Cambridge University Press, Cambridge, 1992).
[16] M. Xu, F. Stefani, and G. Gerbeth, e-print astro-ph/0301321.